




RESEARCH ARTICLE

Synthesis, crystal structure, and Hirschfeld surface analysis of novel ethyl 5-bromo-2-(4-methoxyphenyl) oxazole-4-carboxylate.

Sheikh Murtuja , Venkatesan Jayaprakash , and Barij Nayan Sinha 

Department of Pharmaceutical Sciences and Technology, Birla Institute of Technology, Jharkhand, India

*Corresponding author. Email: murtzasheikh09@gmail.com

Abstract

A new oxazole derivative, ethyl 5-bromo-2-(4-methoxyphenyl) oxazole-4-carboxylate, was synthesized and characterized by IR spectroscopy, ^{13}C NMR, mass spectroscopy, and single-crystal X-ray diffraction analysis. The asymmetric unit of the title compound has two independent molecules (A and B) arranged in an inverted planar orientation, stabilized by intramolecular C-H \cdots O and C-H \cdots N hydrogen bonds and intermolecular C-H \cdots O hydrogen bonds. The crystallographic parameter for the structure $\text{C}_{13}\text{H}_{12}\text{BrNO}_4$ is $M = 326.15$ g/mol, monoclinic, sp. gr. $\text{P}2_1/\text{n}$ (no. 14), $a = 14.828(2)$ Å, $b = 7.1335(9)$ Å, $c = 25.119(2)$ Å, $\beta = 100.066(11)^\circ$, $V = 2616.1(6)$ Å 3 , $Z = 8$. Hirschfeld surface analysis and two-dimensional fingerprint plots provided insights into the short intermolecular interactions, and it was found that H \cdots H (34.4%) interactions contributed the most to the intermolecular interactions. In contrast, the contribution of C \cdots C (2.5%) was the least among all interactions.

Keywords: Oxazole; Hirschfeld surface analysis; π - π stacking interactions; Crystal structure; intermolecular interactions

1. Introduction

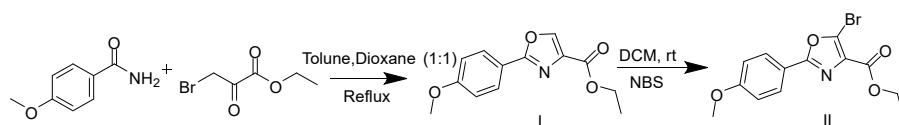
Oxazoles have been previously reported as antibacterial [1–6], anticancer [7–10], antifungal [1, 11, 12], antioxidative [13, 14], antiparasitic [15–17], anti-tubercular [18–21], and antiviral [22–30] agents, and various oxazole derivatives have been synthesized, and their potential in various disease states has been explored. We

synthesized a few oxazole derivatives as part of a project on DENV protease inhibitors. In this communication, we report the synthesis protocol, characterization, Hirschfeld surface analysis, and X-ray crystallographic profile of the synthesized oxazole moiety.

2. Materials and methods

Reagent-grade chemicals and solvents were purchased from CDH, Merck, Sigma, Alfa Aesar, or Rankem. The reaction completion was monitored on normal-phase pre-coated silica using aluminium back-TLC plates (Merck KGaA, Darmstadt, Germany). The melting point was determined using an OPTIMELT automated system and uncorrected.

The two-step synthetic protocol is outlined in Scheme 1



Scheme 1. Reagents and conditions for the synthesis of Scheme 1.

2.1 Procedure for synthesis of ethyl 2-(4-methoxyphenyl) oxazole-4-carboxylate (I)

To a solution of 4-methoxy benzamide (250 mg, 1.65 mmol) and in toluene/dioxane (1:1) (20 ml) at 23° C, ethyl bromopyruvate (0.625 ml, 4.98 mmol) was added, and the reaction mixture was heated to reflux while stirring for 24 h. After confirming the completion of the reaction using TLC, the mixture was cooled to room temperature and concentrated under a vacuum. The residue was extracted using ethyl acetate and washed with brine. The organic layer was then dried over sodium sulfate. The crude product was purified by silica gel column chromatography using Petroleum ether: ethyl acetate (97:3) to yield compound I, ethyl 2-(4-methoxyphenyl) oxazole-4-carboxylate [31]. Yield: 50%, m.p 100–102°C.

2.2 Procedure for synthesis of ethyl 5-bromo-2-(4-methoxyphenyl)oxazole-4-carboxylate (II)

N-Bromosuccinimide (50 mg, 0.202 mmol) was added to a solution of ethyl 2-(4-methoxyphenyl) oxazole-4-carboxylate (10 mL) in a bottom flask, N-bromosuccinimide (126 mg, 0.708 mmol) was added, and the reaction was stirred for 72 h at room temperature, after which the reaction was confirmed by TLC, and the crude product was purified by silica gel column chromatography using petroleum ether: ethyl acetate (96:4) to yield compound II, ethyl 5-bromo-2-(4-methoxyphenyl) oxazole-4-carboxylate. Yield: 85%, m.p 126–128°C.

2.3 Characterization

The FTIR spectra of the title compound were recorded on an IR prestige 21, SHI-MADZU spectrophotometer (Shimadzu Corporation, Japan) in the range of 400–4000 cm^{-1} using KBr pellets. ^1H NMR and ^{13}C NMR spectra of the title compound were

recorded on a JEOL JNM-ECZ 400S/L1 400 MHz NMR spectrometer (JEOL Ltd, Akishima, Tokyo, Japan), and the mass spectra were recorded on a Thermo Scientific Ultimate 3000 spectrometer (Thermo Fisher Scientific, Waltham, Massachusetts, United States) using electrospray ionization mass spectrometry (ESI-MS).

Pale yellow crystalline solid; Yield: 85%, m.p 126–128°C; IR (film) 2920 (C-H, Ar), (C-H, methyl) 2857, (C=O, ester) 1704, (C=C, Ar) 1606, (C=C, Ar) 1546, (C-O, ether) 1248, (C-O, ether) 1066, (C-Br) 518 cm^{-1} ; $^1\text{H-NMR}$ (400 MHz, CHLOROFORM-D) δ 1.40 (t, $J = 7.1$ Hz, 3H), 3.85 (s, 3H) 4.42 (q, $J = 7.1$ Hz, 2H), 6.95 (d, $J = 8.8$ Hz, 2H), 7.97 (d, $J = 9.3$ Hz, 2H); $^{13}\text{C-NMR}$ (101 MHz, CHLOROFORM-D) δ 14.4, 55.6, 61.7, 114.5, 118.4, 128.5, 129.8, 141.1, 160.7, 162.3, 177.5; (m/z): 325.97 $[\text{M}]^+$

$^1\text{H-NMR}$ (400 MHz, CHLOROFORM-D) δ 1.40 (t, $J = 7.1$ Hz, 3H) corresponds to the triplet due to the CH_2 group of the ester, 3.85 (s, 3H) corresponds to the singlet of the CH_3 group of the methoxy group on the aromatic ring, 4.42 (q, $J = 7.1$ Hz, 2H) corresponds to the resonance offered by the CH_3 group of the ester; the four aromatic protons showed resonance at 6.95 (d, $J = 8.8$ Hz, 2H), 7.97 (d, $J = 9.3$ Hz, 2H). The ^{13}C NMR spectral properties corresponded to the structure of the molecule, wherein the δ values of the aliphatic and aromatic carbons were in their expected ranges.

2.4 X-ray crystallographic data collection and structure refinement

X-ray quality single crystals of ethyl 5-bromo-2-(4-methoxyphenyl) oxazole-4-carboxylate (**II**) were obtained by dissolving the sample in a hot petroleum ether and ethyl acetate (95:5) solution, followed by slow cooling at room temperature. Crystals of suitable dimensions were mounted on a Rigaku Oxford Diffraction X-Calibur CCD system, controlled with user-inspired CrysAlis^{Pro} for crystallographic data acquisition with a layer of light mineral oil, and measurements were made using an EnrafNonius Kappa CCD diffractometer with Mo $\text{K}\alpha$ radiation (0.71073 Å). Using Olex-2 [32], the structure was solved using the Olex2.solve [33] structure solution program using charge flipping and refined with the SHELEXL [34] refinement package using least-squares minimization. ORTEP-3 for Windows [35] and Mercury [36] were used to display the stereo diagram and packing display.

The crystal crystallised in the monoclinic P21/n space group, with eight molecules in the unit cell, and the asymmetric unit comprised two independent molecules (A and B) stacked in an inverted orientation (**Fig. 1**). The phenyl rings of molecules A (C2–C7) and B (C15–C20) have a dihedral angle of 15.5(3)°, whereas the oxazole rings of molecules A and B have a dihedral angle of 5.4(3)°, indicating that both molecules (A and B) appear to be nearly coplanar with each other, and the oxazole and phenyl rings within the molecule have dihedral angles of 14.2(3)° and 4.5(3)°, respectively, in molecules A and B. Based on this information, molecule B appears more planar than molecule A. In the crystal, the molecular structure is stabilised by intramolecular C-H...N and C-H...O hydrogen bonding (**Table 1**), and the two molecules of the asymmetric unit are linked by C-H...O intermolecular hydrogen bonding and exhibit a π - π interaction between the sp^2 hybridized carbons of molecules A and B at distances of 3.374 Å and 3.375 Å, respectively, for C4–C22 and C3–C24 interactions, thus forming the A–B unit.

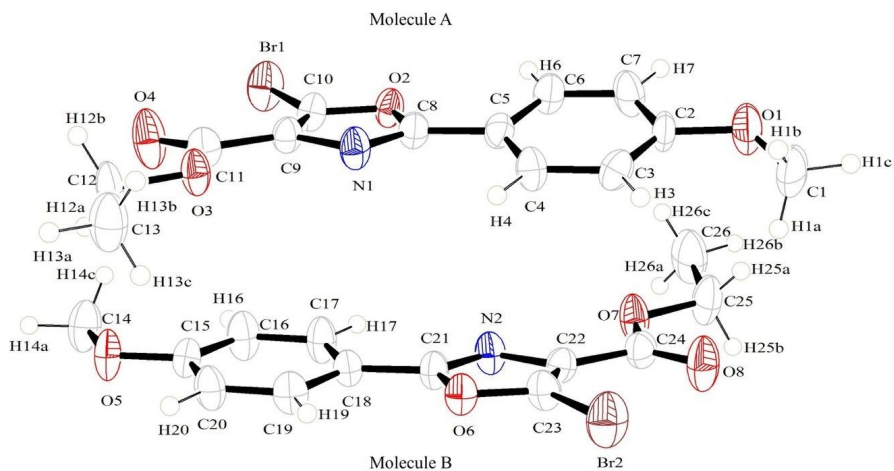


Figure 1. ORTEP diagram of compound II with ellipsoids at the 50% probability level.

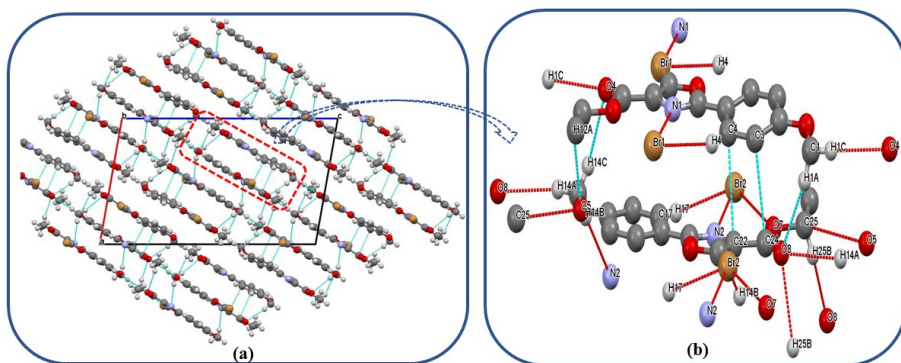


Figure 2. (a). Crystal packing of compound II along the *b*-axis (b). Close view of inter- & intra-molecular interactions made by the asymmetric unit atoms, only those H atoms are shown which are involved in bond formation. (as viewed in the Mercury program)

Table 1. Hydrogen bond geometry (Å) [Compound II]

D-H...A ⁱ	D-H (Å)	H...A (Å)	D...A (Å)	D-H...A [°]
C4-H4...N1 ⁱ	0.93	2.71	2.984 (9)	98.0
C6-H6...O2 ⁱ	0.93	2.51	2.827 (8)	99.9
C17-H17...N2 ⁱ	0.93	2.66	2.962 (9)	99.4
C19-H19...O6 ⁱ	0.93	2.52	2.829 (8)	100.0
C12-H12A...O5 ⁱ	0.97	2.85	3.709	147.85
C14-H14C...O4 ⁱ	0.96	2.86	3.652	139.77
C1-H1A...O8 ⁱ	0.96	2.71	3.623	157.67
C14-H14A...O8 ⁱⁱ	0.96	2.80	3.72	161.20
C1-H1C...O4 ⁱⁱⁱ	0.96	2.76	3.676	158.01
C25-H25B...O8 ⁱⁱⁱ	0.97	2.90	3.67	137.46
C14-H14B...N2 ^{iv}	0.96	2.66	3.85	175.2

The packing in the crystal assumes a layer-like arrangement when viewed along the b-axis, as seen in **Fig. 2**, and the molecules adopt an extended conformation evident from the torsion angles of C11-03-C12-C13=177.2(7)° and C24-07-C25-C26=169.5(8)° respectively for molecules A and B. Further, the crystal packing along the layers is stabilised by intermolecular C-H...O hydrogen bonding and intermolecular O-C interaction with a bond distance of 3.22 Å between the molecules also between the layers, intermolecular C-H...N and C-H...O hydrogen bonding contribute to the stacking arrangement. In addition, the bromine atoms in molecules A and B interact with nitrogen, hydrogen, and oxygen atoms to stabilise the layered packing. Table 2 provides the crystallographic data and structure refinement statistics, and Tables 3 and 4 provide the bond length and bond angle information.

Table 2. Crystallographic data X-ray data collection and structure refinement statistics for the structure C₁₃H₁₂BrNO₄

Empirical formula	C ₁₃ H ₁₂ BrNO ₄
Formula weight	326.15
T/K	295.15
Crystal system, sp.gr., Z	Monoclinic, P2 ₁ /n, 8
a, b, c (Å)	14.828(2), 7.1335(9), 25.119(2)
α, β, γ (deg)	90, 100.066(11), 90
V/Å ³	2616.1(6)
ρ (g/cm ³)	1.656
μ (mm ⁻¹)	3.152
F (000)	1312.0
Crystal size (mm ³)	0.3 × 0.2 × 0.1
Radiation, λ (Å)	MoKα, 0.71073
2θ range for data collection (deg)	6.59 to 49.998
Index ranges	-17 ≤ h ≤ 17, -8 ≤ k ≤ 8, -23 ≤ l ≤ 29
Reflections collected	14007
Independent reflections	4577 [R _{int} = 0.0367, R _σ = 0.0389]
Data/restraints/parameters	4577/0/347
Goodness-of-fit on F ²	1.151
Final R indexes [I ≥ 2σ (I)]	R ₁ = 0.0781, wR ₂ = 0.1961

¹Symmetry code: i=x, y, z; ii=-1/2+x, 1.5-y, -1/2+z; iii=1.5-x, -1/2+y, 1.5-z; iv=1-x, 2-y, 1-z

Empirical formula	C ₁₃ H ₁₂ BrNO ₄
R indexes [all data]	R ₁ = 0.1024, wR ₂ = 0.2140
Largest diff. peak and hole (e Å ⁻³)	0.74/-0.77

Table 3. Selected bond lengths *d* (Å) of compound II

Bond	<i>d</i> , Å	Bond	<i>d</i> , Å
Br1-C10	1.835(7)	Br2-C23	1.823(7)
O2-C10	1.349(8)	O6-C21	1.382(8)
O2-C8	1.385(8)	O6-C23	1.345(8)
O3-C11	1.321(9)	O7-C24	1.321(9)
O3-C12	1.461(8)	O7-C25	1.466(8)
O1-C2	1.373(8)	O8-C24	1.198(8)
O1-C1	1.417(10)	O5-C15	1.361(8)
O4-C11	1.218(9)	O5-C14	1.421(9)
N1-C9	1.394(9)	N2-C22	1.401(8)
N1-C8	1.290(9)	N2-C21	1.295(9)
C10-C9	1.356(9)	C22-C23	1.361(9)
C5-C8	1.460(9)	C22-C24	1.489(9)
C5-C6	1.399(10)	C21-C18	1.459(9)
C5-C4	1.379(10)	C18-C17	1.379(10)
C9-C11	1.464(9)	C18-C19	1.402(10)
C6-C7	1.378(10)	C17-C16	1.386(10)
C4-C3	1.394(10)	C15-C20	1.383(10)
C3-C2	1.381(10)	C15-C16	1.390(10)
C2-C7	1.372(11)	C20-C19	1.363(10)
C12-C13	1.512(11)	C25-C26	1.456(13)

Table 4. Selected bond angles ω (°) of compound II

Angle	ω , deg	Angle	ω , deg
C10-O2-C8	104.2(5)	C23-O6-C21	104.5(5)
C10-C9-N1	108.0(6)	O7-C24-C22	111.8(6)
C10-C9-C11	126.4(6)	C24-O7-C25	115.1(6)
C11-O3-C12	115.4(5)	O8-C24-O7	125.9(7)
C2-O1-C1	119.6(6)	C15-O5-C14	118.5(6)
O2-C8-C5	117.3(6)	O8-C24-C22	122.3(7)
C8-N1-C9	105.4(6)	C21-N2-C22	103.8(6)
N1-C8-O2	113.2(6)	C18-C17-C16	122.0(7)
N1-C8-C5	129.5(7)	O5-C15-C20	116.7(6)
O2-C10-Br1	115.5(5)	O5-C15-C16	124.0(7)
O2-C10-C9	109.3(6)	N2-C22-C24	124.0(6)
C9-C10-Br1	135.2(5)	C20-C15-C16	119.3(6)
C7-C6-C5	119.5(7)	C23-C22-N2	109.1(6)
O3-C11-C9	112.5(6)	C19-C20-C15	121.7(7)
O4-C11-O3	123.5(6)	C23-C22-C24	126.7(6)
C6-C5-C8	120.8(7)	N2-C21-O6	114.1(6)
O4-C11-C9	124.0(7)	O6-C21-C18	117.4(6)
C4-C5-C8	119.8(6)	C20-C19-C18	119.7(7)
C5-C4-C3	120.6(7)	N2-C21-C18	128.5(7)
C4-C5-C6	119.4(6)	C17-C18-C21	120.0(6)

Angle	ω , deg	Angle	ω , deg
C2-C3-C4	119.2(7)	C17-C16-C15	118.7(7)
O1-C2-C3	123.9(7)	C17-C18-C19	118.4(6)
C7-C2-O1	115.8(7)	C19-C18-C21	121.5(6)
C7-C2-C3	120.3(6)	O6-C23-Br2	116.6(5)
C2-C7-C6	120.9(7)	O6-C23-C22	108.5(6)
O3-C12-C13	108.2(6)	C22-C23-Br2	134.9(5)
N1-C9-C11	125.6(6)	C26-C25-O7	108.5(6)

2.5 Refinement

All non-hydrogen atoms were refined using anisotropic thermal parameters. All the H atoms were placed in the calculated positions with C-H= 0.93 Å to 0.97 Å and allowed to refine the structure in riding motion approximations, in which U_{iso} was tied to the carrier atom, with fixed isotropic displacement parameters: U_{iso} (H)=1.5Ueq(C) for methyl groups and U_{iso} (H)=1.2 eq(C) for C aromatic.

2.6 Hirschfeld Surface Analysis

Hirschfeld surface analysis [37] and two-dimensional fingerprint plots [38] were generated using *Crystal Explorer 17.5* [39], which indicated significant interactions based on the d_i and d_e plots. Here, d_i (along the X-axis) and d_e (along the Y-axis) represent the closest internal and external distances on the Hirschfeld surface. The Hirschfeld surfaces of the title compound (**II**) were mapped over the d_{norm} (a), shape index (b), and curvedness index (c). The shape index plot shows π - π stacking interactions, whereas the curvedness plots show surface patch characteristics of planar stacking (Fig. 3).

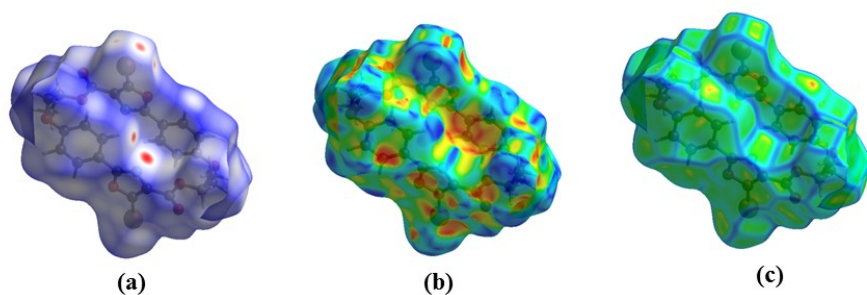


Figure 3. Hirschfeld surfaces of compound (**II**) mapped over d_{norm} (a), shape index (b), and curvedness index (c)

Intermolecular interactions are shown by red-coloured areas [40, 41]. Short interatomic interactions, like hydrogen bonds, are indicated by dark red colour on the d_{norm} surface, while light red indicates other intermolecular interactions.

In the two-dimensional fingerprint plot, the frequency of occurrence of the (d_i d_e) pair is shown in blue, and the grey colour corresponds to the outline of the full fingerprint [42]. The fingerprint plots of compound **II** (Fig. 4) revealed that

H...H (34.4%) was the most prevalent interaction among all other interactions in the compound of interest. Further, the contributions follow the following order in the entire lattice, O...H (20.1%) > C...H (12.3%) > Br...H (10.3%) > N...H (3.7%) > C...C (2.5 %). The C...C interactions correspond to the small π - π stacking interactions observed between the sp^2 hybridized (C4-C22 and C3-C24) carbons of molecules A and B.

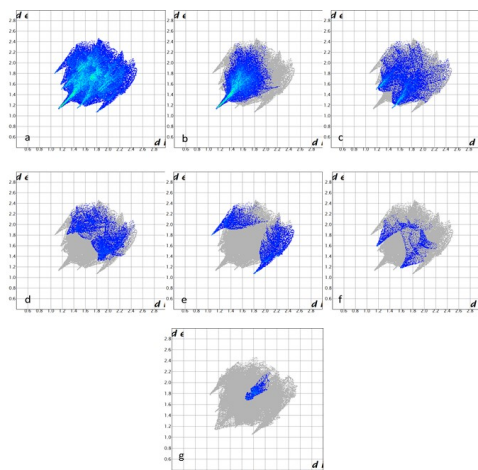


Figure 4. Two-dimensional fingerprint plots of compound (II) showing different interactions with their respective contributions. All interactions (100%) b H...H (34.4%) c C...H (12.3%), d. O...H (20.1%), e. Br...H (10.3%), f. N...H (4.7%), g. C...C (2.5%).

3. Conclusion

Ethyl 5-bromo-2-(4-methoxyphenyl) oxazole-4-carboxylate was synthesized using the method depicted in Scheme I and crystallized using Petroleum ether and ethyl acetate (95:5) solution. Further molecules were characterized by TLC, melting point, IR, NMR, and mass spectroscopy. The asymmetric unit with two molecules was stabilized by C-H...O and C-H...N intramolecular hydrogen bonding and C-H...O intermolecular hydrogen bonding along with π - π stacking interactions offered by the sp^2 hybridized carbons. Furthermore, the Hirshfeld surface analysis revealed that, in the lattice, H...H (34.4%) was the most prevalent interaction, while C...C interactions contributed the least to the intermolecular interaction profile, with a contribution of 2.5% in the entire lattice.

4. Declarations

4.1 Acknowledgements

The authors are thankful to the funding agency DST-SERB, Govt. of India, for providing financial assistance through their project (EMR/2016/005711) dated August 7, 2017, and to Birla Institute of Technology, Mesra, Ranchi, India, for providing the

NMR spectral facility at the Chemistry Department through the DST FIST program (SR/FST/CSI-242-2012) and CIF for providing the single-crystal X-ray diffraction facility and other analytical services. Further, the authors sincerely acknowledge the support of Dr Swaraj Sengupta from the Department of Chemical Engineering, Birla Institute of Technology, Mesra, in refining the crystal structure.

4.2 Ethics approval and consent to participate

Not applicable.

4.3 Consent for publication

Not applicable.

4.4 Availability of data and materials

Crystallographic data were deposited with the Cambridge Crystallographic Data Centre as a supplementary publication with CCDC 2062478 for 5-bromo-2-(4-methoxyphenyl) oxazole-4-carboxylate. The data can be obtained free of charge from the Cambridge Crystallographic Data Center via <https://www.ccdc.cam.ac.uk/>

4.5 Competing interests

The authors declare that they have no competing interests.

4.6 Funding

The authors thank the funding agency DST-SERB, Govt. of India, for providing financial assistance through their project (EMR/2016/005711) dated August 7, 2017.

4.7 Author contributions

The authors confirm their contribution to the paper as follows: *Study conception and design*: S Murtuja; *Data collection*: S Murtuja; *Analysis and interpretation of results*: S Murtuja, V Jayaprakash, BN Sinha; *Draft manuscript preparation*: S Murtuja. All authors reviewed the results and approved the final version of the manuscript.

References

- (1) Tomi, I. H. R.; Tomma, J. H.; Al-Daraji, A. H. R.; Al-Dujaili, A. H. *J Saudi Chem Soc* **2015**, *19*, 392–398.
- (2) Škedelj, V. et al. *Eur J Med Chem* **2013**, *67*, 208–220.
- (3) Li, N. et al. *Bioorganic Med Chem Lett* **2014**, *24*, 386–389.
- (4) Stokes, N. R. et al. *Bioorganic Med Chem Lett* **2014**, *24*, 353–359.
- (5) Prakash, T. B.; Reddy, G. D.; Padmaja, A.; Padmavathi, V. *Eur J Med Chem* **2014**, *82*, 347–354.
- (6) Patil, P. C.; Tan, J.; Demuth, D. R.; Luzzio, F. A. *Bioorganic Med Chem* **2016**, *24*, 5410–5417.
- (7) Bell, J. L.; Haak, A. J.; Wade, S. M.; Kirchoff, P. D.; Neubig, R. R.; Larsen, S. D. *Bioorganic Med Chem Lett* **2013**, *23*, 3826–3832.
- (8) Naud, S. et al. *J Med Chem* **2013**, *56*, 10045–10065.
- (9) Rafferty, S. W.; Eisner, J. R.; Moore, W. R.; Schotzinger, R. J.; Hoekstra, W. J. *Bioorganic Med Chem Lett* **2014**, *24*, 2444–2447.
- (10) Zhu, H. Y.; Desai, J.; Deng, Y.; Cooper, A.; Wang, J.; Shipps, J.; Samatar, A.; Carr, D.; Windsor, W. *Bioorganic Med Chem Lett* **2015**, *25*, 1627–1629.
- (11) Pedras, M. S. C.; Abdoli, A. *Bioorganic Med Chem* **2013**, *21*, 4541–4549.
- (12) Zhang, M.-Z.; Chen, Q.; Xie, C.-H.; Mulholland, N.; Turner, S.; Irwin, D.; Gu, Y.-C.; Yang, G.-F.; Clough, J. *Eur J Med Chem* **2015**, *92*, 776–783.
- (13) De la Fuente Revenga, M.; Fernández-Sáez, N.; Herrera-Arozamena, C.; Morales-García, J. A.; Alonso-Gil, S.; Pérez-Castillo, A.; Caignard, D.-H.; Rivara, S.; Rodríguez-Franco, M. I. *J Med Chem* **2015**, *58*, 4998–5014.
- (14) Gobec, M.; Tomašič, T.; Markovič, T.; Mlinarič-Raščan, I.; Dolenc, M. S.; Jakopin, Ž. *Chem Biol Interact* **2015**, *240*, 200–207.
- (15) Chakka, S. K.; Kalamuddin, M.; Sundararaman, S.; Wei, L.; Mundra, S.; Mahesh, R.; Malhotra, P.; Mohammed, A.; Kotra, L. P. *Bioorganic Med Chem* **2015**, *23*, 2221–2240.
- (16) Ferrins, L. et al. *Eur J Med Chem* **2013**, *66*, 450–465.
- (17) Yamamuro, D.; Uchida, R.; Ohtawa, M.; Arima, S.; Futamura, Y.; Katane, M.; Homma, H.; Nagamitsu, T.; Osada, H.; Tomoda, H. *Bioorganic Med Chem Lett* **2015**, *25*, 313–316.
- (18) Abhale, Y. K.; Sasane, A. V.; Chavan, A. P.; Shekh, S. H.; Deshmukh, K. K.; Bhansali, S.; Nawale, L.; Sarkar, D.; Mhaske, P. C. *Eur J Med Chem* **2017**, *132*, 333–340.
- (19) Franke, J.; Bock, M.; Dehn, R.; Fohrer, J.; Mhaske, S. B.; Migliorini, A.; Kanakis, A. A.; Jansen, R.; Herrmann, J.; Müller, R.; Kirschning, A. *Chem - A Eur J* **2015**, *21*, 4272–4284.
- (20) Li, D.; Gao, N.; Zhu, N.; Lin, Y.; Li, Y.; Chen, M.; You, X.; Lu, Y.; Wan, K.; Jiang, J.-D.; Jiang, W.; Si, S. *Bioorganic Med Chem Lett* **2015**, *25*, 5178–5181.
- (21) Meissner, A.; Boshoff, H. I.; Vasan, M.; Duckworth, B. P.; Barry, C. E.; Aldrich, C. C. *Bioorganic Med Chem* **2013**, *21*, 6385–6397.
- (22) Belema, M.; Nguyen, V.; Romine, J.; Laurent, D.; Lopez, O.; Goodrich, J. *J Med Chem* **2014**, *57*, 1995–2012.
- (23) Draffan, A.; Frey, B.; Fraser, B.; Pool, B.; Gannon, C.; Tyndall, E. *Bioorganic Med Chem Lett* **2014**, *24*, 4984–4988.
- (24) Keaney, E. P.; Connolly, M.; Dobler, M.; Karki, R.; Honda, A.; Sokup, S.; Karur, S.; Britt, S.; Patnaik, A.; Raman, P.; Hamann, L. G.; Wiedmann, B.; LaMarche, M. J. *Bioorganic Med Chem Lett* **2014**, *24*, 3714–3718.
- (25) Kim, S.-H.; Markovitz, B.; Trovato, R.; Murphy, B. R.; Austin, H.; Willardsen, A. J.; Baichwal, V.; Morham, S.; Bajji, A. *Bioorganic Med Chem Lett* **2013**, *23*, 2888–2892.
- (26) Regueiro-Ren, A. et al. *J Med Chem* **2013**, *56*, 1656–1669.

- (27) Sevrioukova, I. F.; Poulos, T. L. *J Med Chem* **2013**, *56*, 3733–3741.
- (28) Laurent, D. R. S. et al. *J Med Chem* **2014**, *57*, 1976–1994.
- (29) Wang, T.; Yang, Z.; Zhang, Z.; Gong, Y.-F.; Riccardi, K. A.; Lin, P.-F.; Parker, D. D.; Rahematpura, S.; Mathew, M.; Zheng, M.; Meanwell, N. A.; Kadow, J. F.; Bender, J. A. *Bioorganic Med Chem Lett* **2013**, *23*, 213–217.
- (30) Zhong, Z.-J.; Zhang, D.-J.; Peng, Z.-G.; Li, Y.-H.; Shan, G.-Z.; Zuo, L.-M.; Wu, L.-T.; Li, S.-Y.; Gao, R.-M.; Li, Z.-R. *Eur J Med Chem* **2013**, *69*, 32–43.
- (31) Raju, B.; Ciabatti, R.; Maffioli, S.; Singh, U.; Romano, G.; Michelucci, E.; Tiseni, P.; Candiani, G.; Kim, B.; O'dowd, H., et al. (LLC, V. P.). Ramoplanin derivatives possessing antibacterial activity US Patent, 20060211603A1, Publisher: Google Patents, 2006.
- (32) V., D. O.; LJ, B.; RJ, G.; JAK, H.; H, P. *J Appl Crystallogr* **2009**, *42*, 339–41.
- (33) Bourhis, L.; V., D. O.; Gildea, R.; Howard, J.; Puschmann, H. *Acta Crystallogr A Found Adv* **2015**, *71*, 59–75.
- (34) Sheldrick, G. *ystallogr Sect C Struct Chem* **2015**, *71*, 3–8.
- (35) Farrugia, L. *J Appl Crystallogr* **2012**, *45*, 849–54.
- (36) Macrae, C.; Bruno, I.; Chisholm, J.; Edgington, P.; McCabe, P.; Pidcock, E. *J Appl Crystallogr* **2008**, *41*, 466–70.
- (37) Spackman, M.; Jayatilaka, D. *CrystEngComm* **2009**, *11*, 19–32.
- (38) McKinnon, J.; Jayatilaka, D.; Spackman, M. *Chem Commun* **2007**, *37*, 3814–3816.
- (39) Spackman, P. R.; Turner, M. J.; McKinnon, J. J.; Wolff, S. K.; Grimwood, D. J.; Jayatilaka, D.; Spackman, M. A. *J Appl Crystallogr* **2021**, *54*, Publisher: International Union of Crystallography, 1006–1011.
- (40) McKinnon, J. J.; Spackman, M. A.; Mitchell, A. S. *Acta Crystallogr B Struct Sci* **2004**, *60*, Pages: 627–68 Volume: 60, 627–668.
- (41) Spackman, M.; McKinnon, J. *CrystEngComm* **2002**, *4*, 378–92.
- (42) Ternavisk, R.; Camargo, A.; Machado, F.; Napolitano, H. *J Mol Model* **2014**, *20*, 2526–2536.